Design Guidelines For Conjugated Polymers With Light-Activated Anticancer Activity

Chengfen Xing, Libing Liu, Hongwei Tang, Xuli Feng, Qiong Yang, Shu Wang,* and Guillermo C. Bazan**

Multifunctional materials that simultaneously provide therapeutic action and image the results provide new strategies for the treatment of various diseases. Here, it is shown that water soluble conjugated polymers with a molecular design centered on the polythiophene–porphyrin dyad are effective for killing neighboring cells. Following photoexcitation, energy is efficiently transferred from the polythiophene backbone to the porphyrin units, which readily produce singlet oxygen ($^1O_2$) that is toxic for the cells. Due to the light-harvesting ability of the electronically delocalized backbone and the efficient energy transfer amongst optical partners, the polythiophene–porphyrin dyad shows a higher $^1O_2$ generation efficiency than a small molecule analog. The fluorescent properties of these polymers can also serve to distinguish amongst living and dead cells. Polymers can be designed with folic acid grafted onto the polymer side chain that can specifically kill folate receptor-overexpressed cells, thereby providing an important demonstration of anticancer specificity through molecular design.

1. Introduction

Conjugated polymers are characterized by a delocalized π-electronic backbone structure and large optical absorption coefficients. Facile energy transfer along the backbone and between chains allows excitations to sample a larger number of environments in comparison to isolated small molecules.[1] Photoexcitations can be channeled to suitable adjacent acceptors by fluorescence resonance energy transfer (FRET) mechanisms, leading to sensitization of emitters to levels above those attained by direct excitation. Conjugated polyelectrolytes (CPEs) incorporate charged groups onto the conjugated polymer backbone. Such a structural modification improves solubility in aqueous media, an important requirement for interacting with biological systems and for the design of optically amplified fluorescent biosensors.[2]

Acceptor molecules can be chosen with optoelectronic properties that optimize FRET efficiencies.[3,4] Water soluble conjugated polymer/acceptor dyads have therefore gained much recent attention in various applications for detection and cell imaging.[5–10] Energy transfer to porphyrin acceptors is a special example whereby the excitations can be harnessed to generate reactive oxygen species[11–14] and enable applications in photodynamic therapy (PDT).[15] Such materials can be expected to act as both therapeutic and imaging agents. The imaging function is particularly significant when it is capable of monitoring and guiding treatment. Integration of reporting modalities with therapeutic function within a single bio-compatible polymer structure is therefore anticipated to increase in importance as a new and challenging design element for new artificial materials.[16,17]

Here, we describe the synthesis and application of polymers containing conjugated polythiophene–porphyrin dyads that were specifically designed to function concurrently as an anticancer agent and an imaging reporter. **Figure 1** shows the first example, PTP, which relies on a *cationic* polythiophene framework. Four significant design characteristics were included in the molecular features. First, the fractional content of porphyrin moieties linked to the polythiophene backbone is low (≈1%), in order to minimize toxicity in the absence of photoexcitation. Second, the amphiphilic attributes were anticipated to promote adsorption to cells through a combination of electrostatic and hydrophobic binding forces. Third, covalent attachment of porphyrin moieties to the light harvesting polythiophene backbone constrains interchromophore distances for optimizing FRET. This design element is important for increasing the photocoversion efficiency of singlet oxygen ($^1O_2$) generation and reducing light intensity requirements. Fourth, because the backbone retains partial emission, it can also be used to monitor apoptosis and necrosis processes by fluorescence imaging, adding a new dimension to the function of the molecular construct. Such simultaneous imaging and PDT function[18,19] extend the applications of water-soluble conjugated polymers beyond their established biosensing capabilities. The PTP platform can

C. Xing, Dr. L. Liu, H. Tang, X. Feng, Dr. Q. Yang, Prof. S. Wang
Beijing National Laboratory for Molecular Science
Key Laboratory of Organic Solids, Institute of Chemistry
Chinese Academy of Sciences
Beijing, 100190, P. R. China
E-mail: liulibing@iccas.ac.cn; wangshu@iccas.ac.cn
Prof. G. C. Bazan
Departments of Chemistry & Biochemistry and Materials
Center for Polymers and Organic Solids
University of California
Santa Barbara, CA 93106-9510, USA
E-mail: bazan@chem.ucsb.edu

DOI: 10.1002/adfm.201100840

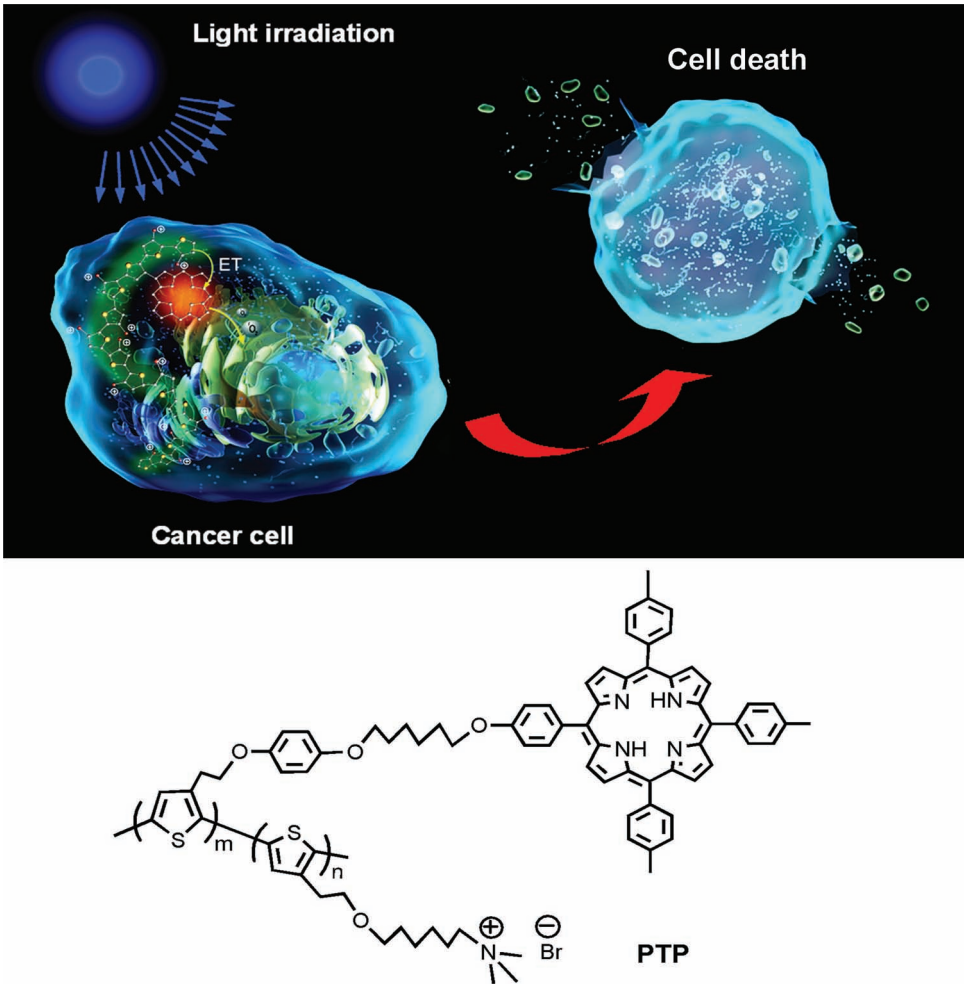

Figure 1. Chemical structure of PTP and a schematic mechanism of PTP anticancer activity under irradiation. Components in the cell are not drawn to scale.

be further modified with molecular fragments that endow the materials with specificity (vide infra).

2. Results and Discussions

Figure 2 shows the synthesis of PTP; complete details can be found in the Supporting Information. Reaction of pyrrole, 4-(6-bromohexyloxy)benzaldehyde (**1**)[20] and *p*-tolualdehyde (**2**) in the presence of BF_3-diethyl ether in $CHCl_3$, followed by treatment with 2,3-dichloro-5,6-dicyanobenzoquinone (DDQ) affords the porphyrin derivative **3**. Treatment of **3** with 30% trimethylamine-methanol solution provides the cationic porphyrin derivative TPN. The quaternary ammonium side chain of TPN improves the polarity and water solubility, and thus TPN is soluble in water. This was proved by the linear plot of TPN absorbance as a function of various concentrations (Figure S1). Monomer **6** was prepared by reaction of 2-(3-thienyl)-ethanol tosylate (**4**) and hydroquinone, followed by reaction with **3**. Reaction of 2-(thiophen-3-yl)ethanol (**7**) with 1,6-dibromohexane in the presence of sodium hydride in dry DMF under nitrogen affords 3-(2-(6-bromohexyloxy)ethyl)thiophene (**8**) in 31% yield. Subsequent conversion to 6-(2-(thiophen-3-yl)ethoxy)hexyltrimethylammonium bromide (**9**) is accomplished in 89% yield by reaction with excess trimethylamine in methanol. The cationic polythiophene PT was obtained through oxidative polymerization of **9** in chloroform using $FeCl_3$, followed by purification by dialysis in water. Monomers **6** and **9** undergo oxidative copolymerization under nitrogen in the presence of $FeCl_3$ to give the target cationic porphyrin-containing polythiophene (PTP). The molar feed ratio of monomer of **6** to **9** is 1:10 and the actual porphyrin content in PTP was determined to be ~1% by examination of the absorption spectrum (Figure S2 in the Supporting Information).

The photophysical properties of PTP, PT and TPN were investigated in aqueous solution, and the most relevant results are shown in **Figure 3**a and 3b. For TPN, the absorption spectrum exhibits a Soret band at 420 nm and Q bands between 520 nm and 670 nm; the emission spectrum shows a maximum peak at 655 nm with a fluorescence quantum yield (QY) of 1%. For PT, the absorption maximum is at ≈420 nm, corresponding to the π–π^* transition of the backbone; emission displays a maximum at 578 nm and occurs with a QY of 2%. The absorption spectrum of PTP incorporates features common to the

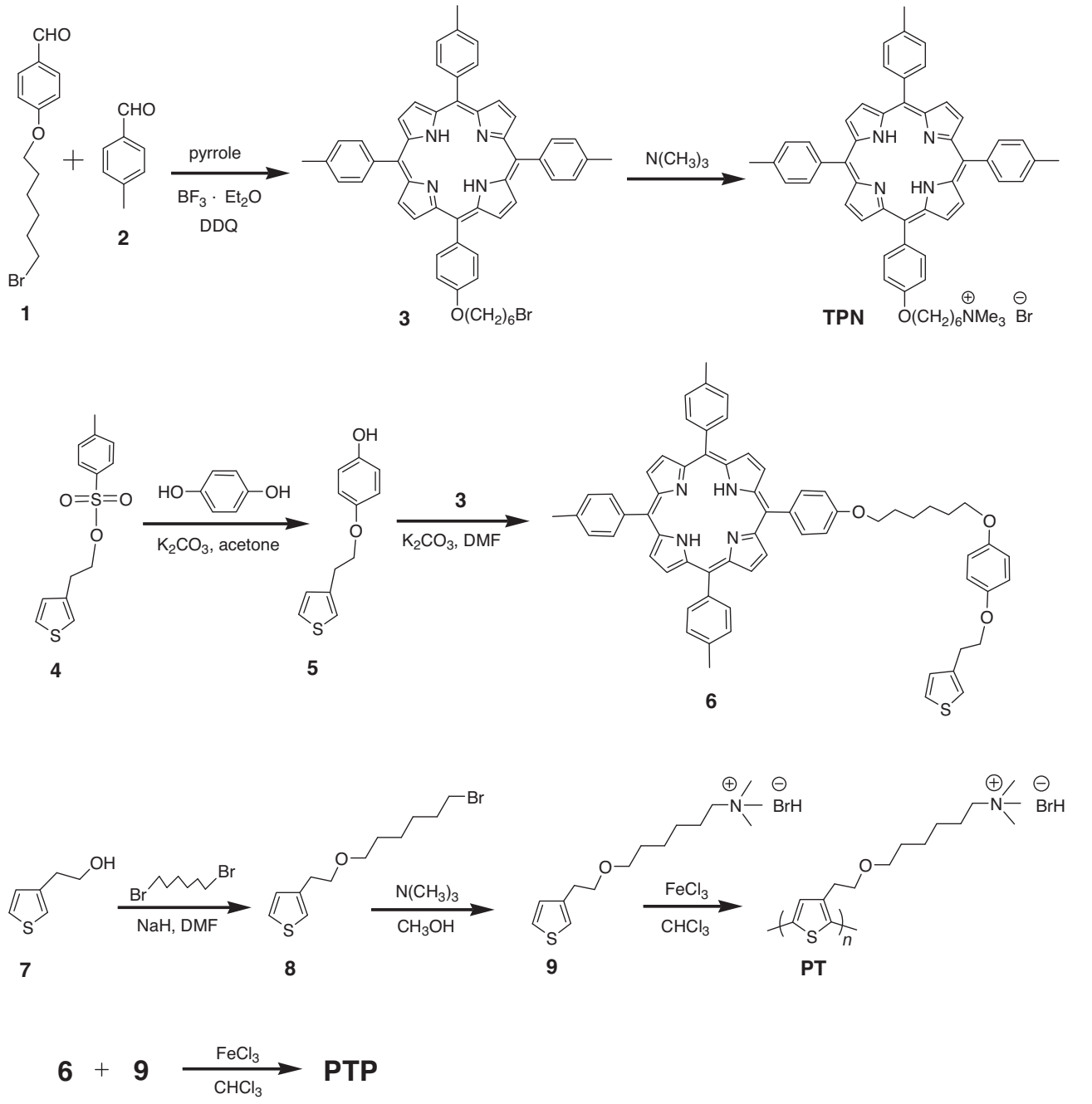

Figure 2. Synthetic preparations of TPN, PT, and PTP.

backbone and the porphyrin units. Excitation of PTP at 470 nm, where the porphyrin units do not absorb, leads to emission with peaks at 578 nm and 658 nm with a QY of 2%. That a peak is observed at 658 nm demonstrates efficient energy transfer from polythiophene units to the porphyrin sites. It is also relevant to note at this point that the hydrophobic component of the PTP structure leads to aggregation in aqueous solution. Dynamic light scattering (DLS) measurement shows that the average particle size is approximately 350 nm (Figure 3c). The size of these nanoparticles is in the appropriate range for improved cell uptake.[21,22]

Relative $^1O_2$ photogeneration efficiencies by the different photosensitizers were probed by measuring the conversion of disodium 9,10-anthracenedipropionic acid (ADPA)[23] to its endoperoxide via the corresponding decrease of the absorption band at 378 nm. PTP, TPN and PT were compared upon exposure to white light (400–800 nm), and the results are summarized in Figure 3d. In these experiments, the concentrations of PT and PTP were 10 μM in terms of polymer repeat units (RUs), and the concentration of TPN (0.15 μM) was similar to that of the pendant porphyrin units in the PTP solutions. The first order plots of the decrease of ADPA absorption at 378 nm

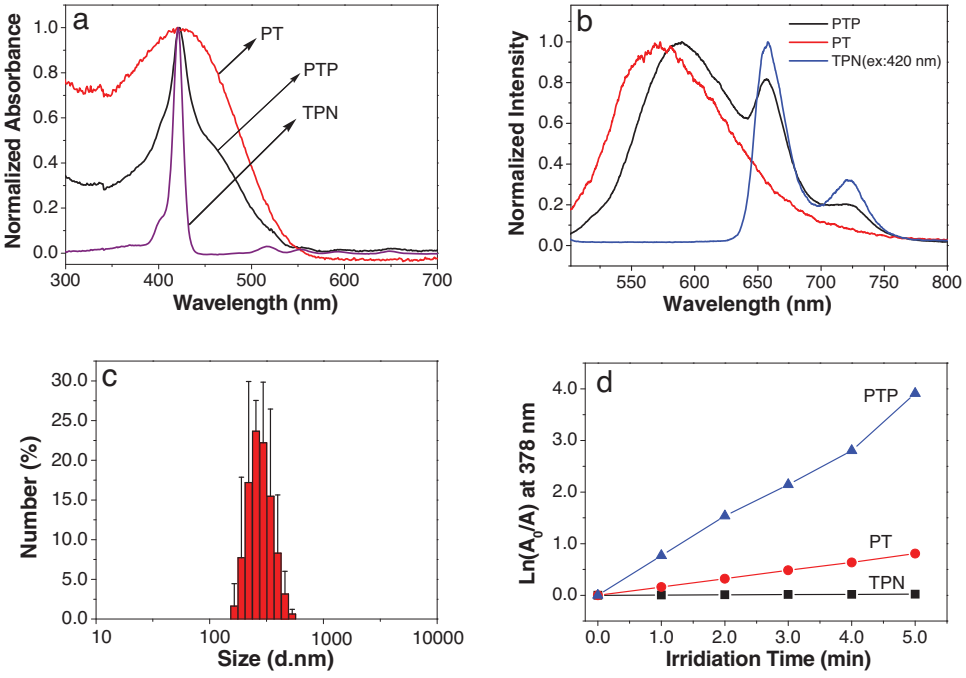

Figure 3. Photophysical properties of PTP, PT and TPN, structural characterization of PTP aggregation in water, and comparison of $^1O_2$ generation efficiencies. a) Normalized UV–vis absorption spectra of PTP, PT and TPN in aqueous solution. b) Normalized emission spectra of PTP, PT and TPN in aqueous solution. PT and TPN were excited at 420 nm and PTP at 470 nm. c) Dynamic light scattering analysis of PTP aggregates in aqueous solution. d) Decrease of ADPA absorption at 378 nm as a function of light irradiation time in the presence of TPN, PT and PTP in D_2O solution. [PTP] = [PT] = 10 μM in RUs, [TPN] = 0.15 μM and [ADPA] = 120 μM. A_0 is the absorbance of ADPA at 378 nm before irradiation, and A is that after irradiation with white light (400–800 nm). Values represent subtraction of the residual bleaching data of ADPA alone under the same irradiation condition.

as a function of irradiation time[14] show faster disappearance upon photoexcitation of PTP. The observed rate constants of ADPA consumption in the presence of PTP, PT and TPN are 1.25×10^{-2}, 2.7×10^{-3} and 7.3×10^{-5} s^{-1}, respectively. Thus, the bleaching rate of ADPA with PTP is 170 fold faster than that with TPN and ≈5 fold faster than that with PT. As control experiment, the production of singlet oxygen by a sample containing both PT and TPN with concentrations matching those of the PTP sample has been evaluated (Figure S3). The observed rate constants of ADPA consumption is 1.6×10^{-3} s^{-1}, one order of magnitude less than that for PTP. Covalent attachment of porphyrin moieties onto PTP thus yields a synergistic improvement relative to the isolated PT or TPN components, and are consistent with energy transfer from the polythiophene backbone to the porphyrin sites, which significantly increases the $^1O_2$ generation efficiency (see also Figure S4 in the Supporting Information).

The ability of PTP to generate $^1O_2$ was anticipated to induce oxidative stress and trigger apoptosis, necrosis or autophagy-associated cell death.[24] Two kinds of cancer cells, pulmonary adenocarcinoma cell (A549) and renal cell carcinoma (A498), were used as initial model targets. The morphologies of A498 cancer cells in the presence of PTP after different periods of illumination were examined by phase contrast and fluorescence microscopy. For these experiments, plates containing A498 cells were irradiated at 470 nm for 0, 10, and 30 min, respectively, ethidium bromide (EB), which only stains apopotic or dead cells, was then added. Resulting samples were examined by fluorescence microscopy by excitation at 470 nm to selectively excite the polythiophene backbone. As shown by the phase contrast bright-field images in **Figure 4**a, irradiation leads to cell morphology changes that include chromatin compaction, cytoplasm condensation, and, more significantly, a large amount of blebbing. After 30 min irradiation, whole-cell shrinkage takes place. Persistent volume reduction is a major hallmark of cell death.[25,26] These results are corroborated by the overlapping fluorescence images of A498 cells in the presence of PTP and EB, where the amount of EB-stained dead cells has increased in tandem with prolonged irradiation time. As shown in Figure 4b, imaging the location of PTP emission can be used to distinguish between living and dead cells. In living cells, the PTP emission is largely located in the cytoplasm. For dead cells, one observes translocation such that the PTP fluorescence now takes place within the nucleus. Correlation with the fluorescence from EB-stained cells confirms assignment of dead cells.

Cytotoxicities of PTP, PT and TPN toward the A498 and A549 cancer cells were determined by using a standard assay in which the conversion of MTT (3-(4,5-dimethylthiazol-2-yl)-2,5-diphenyl-2H-tetrazolium hydrobromide) into formazan is related to mitochondrial activity and thereby cell viability.[27] The PDT treatment was performed by illumination at 470 nm for 30 min. As shown in Figure 4c, under illumination, PTP displays more prominent cytotoxicity than PT at similar repeat unit concentrations, and TPN (normalized to the molar quantity of pendant porphyrin units). Also noteworthy is that PTP exhibits very low dark cytotoxicity, which is similar to PT and TPN (Figure S5). Moreover,

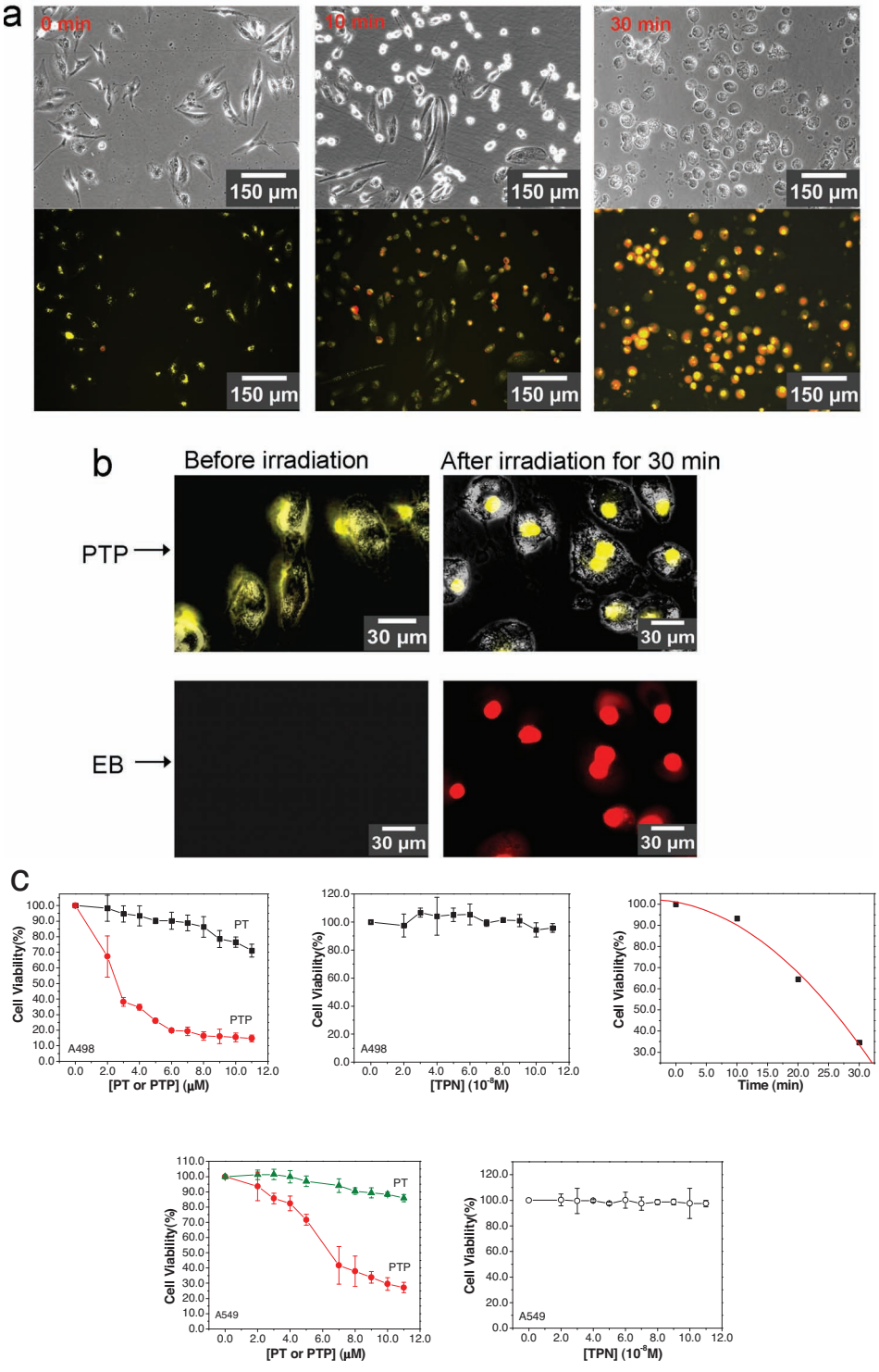

Figure 4. Apoptosis and imaging of A498 and A549 cancer cells by PTP upon irradiation at 470 nm with a 2.5 J ·cm^{-2} source. a) Phase contrast bright-field images (upper) of A498 cells upon light irradiation from 0 to 30 min in the presence of PTP and overlapping fluorescence images of A498 cells (bottom) under PTP and EB filters. Phase contrast images were taken at 100 ms and the fluorescence images were taken at 300 ms under PTP and EB filters. The magnification of objective lens is 10×. b) Overlapping images of A498 cancer cells under phase contrast bright field and under fluorescence field for PTP and EB before and after 30 min irradiation. The magnification of objective lens is 40×. The false color of PTP is yellow and the type of light filter is D455/70 nm exciter, 500 nm beamsplitter, and D525/30nm emitter. The false color of EB is red and the type of light filter is D540/40 nm exciter, 570 nm beamsplitter, and D600/50 nm emitter. c) Dose-response curve data for cell viability of A498 and A549 cells treated with PTP, PT and TPN by using a typical MTT assay under 470 nm light irradiation for 30 min, and the cell viability of A498 cell treated with [PTP] = 10 μM versus different durations of light exposure. Error bars correspond to standard deviations from three separate measurements.

a lower light dose at a fluence rate of 1.4 mW·cm^{-2} for 30 min of irradiation (2.5 J·cm^{-2}) is used in our PDT experiment, which compares well to the performance parameters of approved photosensitizers.[17,28,29] We also examined the decrease of A498 cell viability with increasing light exposure time by the MTT assay (Figure 4c) at [PTP] = 10 μM RUs. The results show that cell viability decreases with increasing illumination time and that significant cell death is induced after 30 min.

Since cells typically exhibit a net negative charge, cationic CPEs bind to their surfaces through electrostatic interactions. While such binding aids in the diffusion across membrane, it makes specific and selective action on a given type of cell difficult to achieve. Subsequent molecular optimization therefore focused on targeting tumor cells by taking advantage of a group capable of selectivity (folic acid) and by removing complications due to electrostatic binding. These considerations led to the design of PTPF shown in **Figure 5**. PTPF is charge neutral, yet water soluble through the integration of pegylated side chains. PTPF also retains the critical optical elements that enable $^1O_2$ generation, as described with PTP. A fractional number of

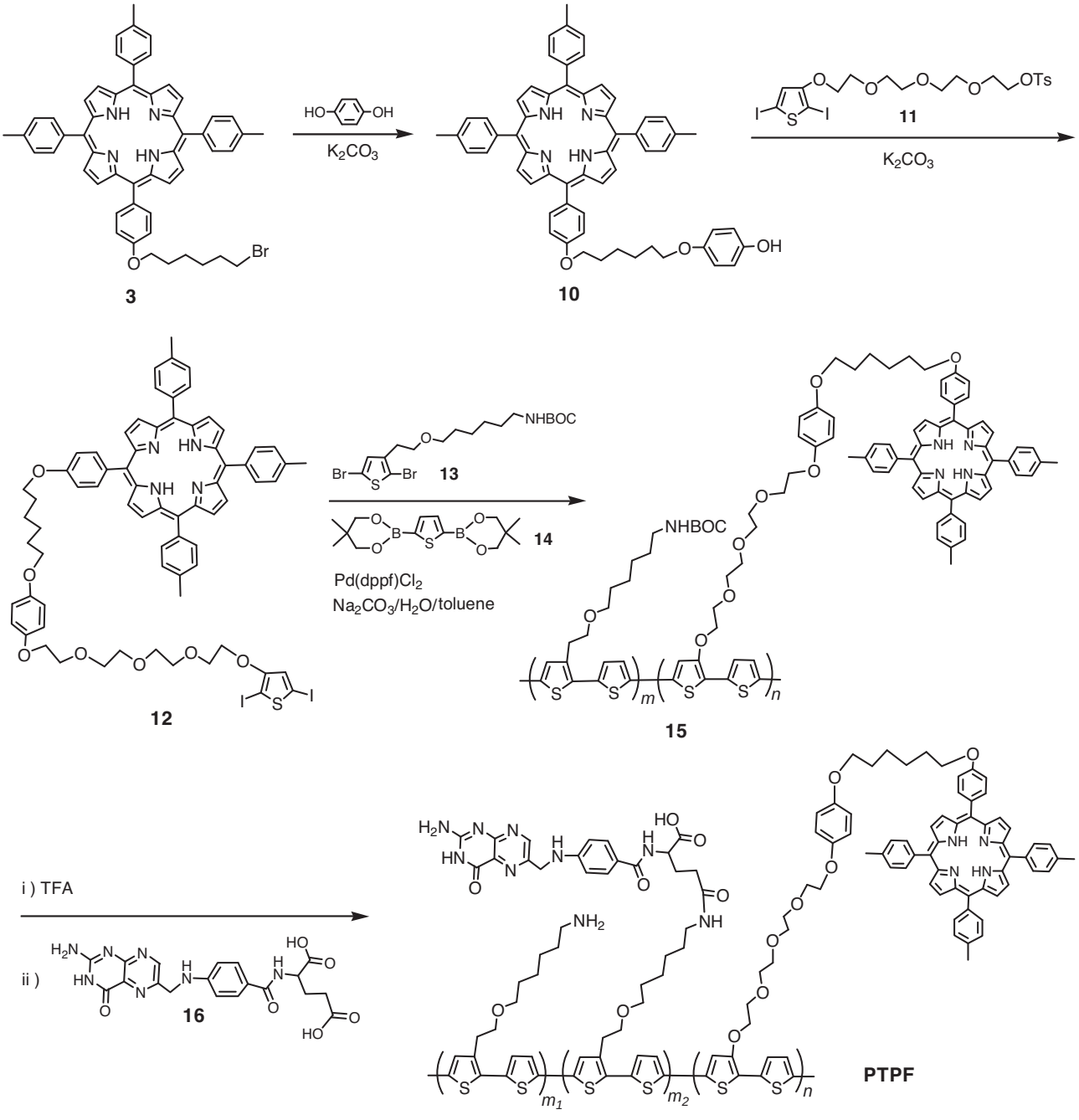

Figure 5. Synthetic preparation of PTPF.

grafted folic acid functionalities were also grafted to the backbone. The rationale behind this incorporation stems from the fact that folate receptor (FR) is a tumor-associated protein that can bind folic acid with high affinity ($K_d \approx 10^{-10}$ M).[30] We thus anticipated that PTPF would preferentially bind and kill FR-overexpressed cancer cells. On this basis, PTPF presents a new design for improving the efficiency of delivering fluorescence imaging and photosensitizers to the desired cancer cell targets with reduced accumulation in normal cells. Synthetic access into PTPF is shown in Figure 5 and all the synthetic procedures are included in the Supporting Materials.

KB cancer cells with over-expressed FR and FR-negative NIH-3T3 fibroblasts cells were chosen as target cells in a set of experiments designed to test the specificity of PTPF. Control tests by Western blot analysis reveals the presence of high levels of FR in the KB cells and little expression in NIH-3T3 cells (see Figure S6 in the Supporting Information). We first examined how PTPF interacts with the cells. Cells were incubated with PTPF (20.0 μg/mL) for 24h, and images were then collected by fluorescence microscopy. **Figure 6**a and 6b show the phase contrast bright-field and fluorescence images of the resulting KB cancer and NIH-3T3 cells. In comparison with NIH-3T3 cells, one can clearly observe more pronounced PTPF accumulation in the KB cells, presumably as a result of the folate receptor-mediated uptake.

Specificity toward KB cancer cells over NIH 3T3 cells was investigated by the MTT assay. In these experiments, KB and NIH-3T3 cells were incubated with PTPF (25.0 μg/mL) for 24 h, followed by either keeping in the dark or exposing to irradiation with 5.0 J/cm^2 light doses at a fluence rate of 2.8 mW·cm^{-2} for 30 min. As shown in Figure 6c, PTPF displays more prominent cytotoxicity against KB cells under light irradiation than in the dark (Figure 6c, left). The viability of KB cells drops below 20% upon irradiation. However, toward NIH-3T3 cells, PTPF only exhibits little cytotoxicity and cell viabilities remain above 70% in the dark or upon irradiation. Also no obvious difference of cell viability was observed for NIH-3T3 cells in the dark and upon irradiation (Figure 6c, right). Furthermore, the role of folate receptors on cell surface in PTPF uptake was assessed by incubating KB cells with PTPF (30.0μg mL^{-1}) in the presence of 2 mM free folic acid used as competitive inhibitor of cellular uptake. As shown in Figure S7, PTPF exhibits little cytotoxicity in the dark and upon light irradiation in the presence of free folic acid. The result shows that the presence of free folic acid effectively inhibits uptake of polymer by the cells. These results show that the photoinduced cytotoxity of PTPF is more effective toward FR-overexpressed cells than FR-negative cells thereby indicating specific anticancer activity.

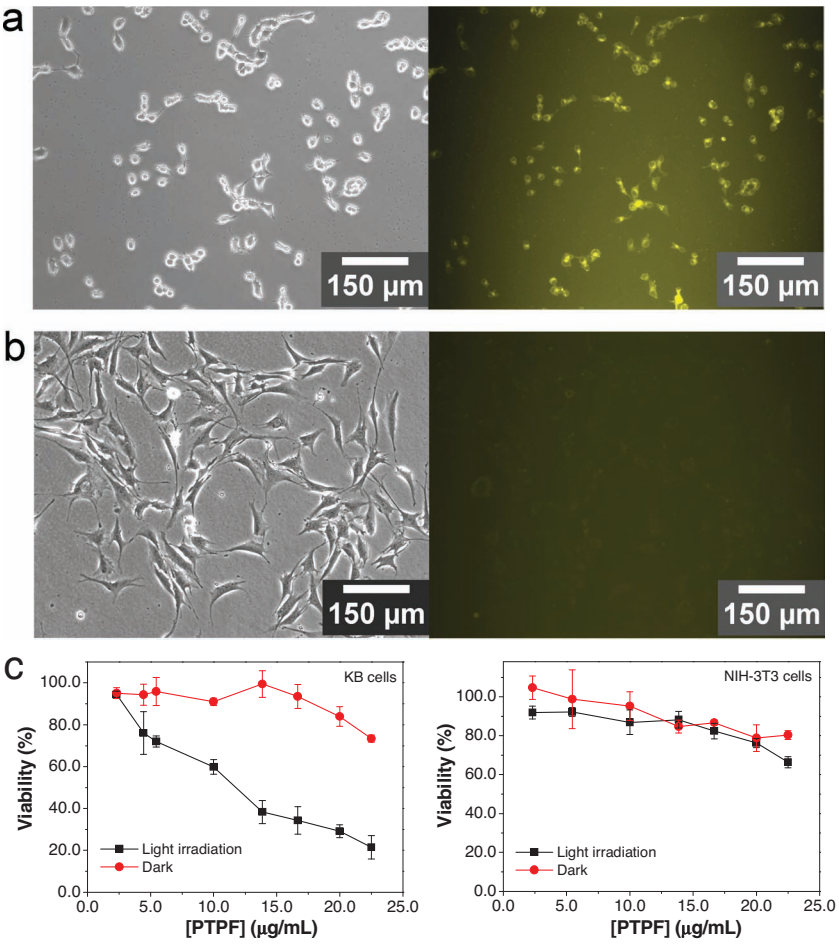

Figure 6. Phase contrast bright-field and fluorescence images of KB cancer cells (a) and NIH-3T3 cells (b) in the presence of PTPF (20.0 μg mL^{-1}). Left: phase contrast bright-field images. Right: fluorescence images. The false color of PTPF is yellow and the type of light filter is D455/70 nm exciter, 500 nm beamsplitter, and D525/30 nm emitter. The magnification of object lens is 10×. c) Dose-response curves for cell viability of KB cells and NIH-3T3 cells treated with PTPF by using a typical MTT assay under 470 nm light irradiation or in the dark. Error bars correspond to standard deviations from three separate measurements.

3. Conclusions

In conclusion, we have designed, synthesized and characterized the therapeutic function of cationic and neutral conjugated water-soluble polymers that comprise a polythiophene backbone and pendant porphyrin chromophores. Excitation of the backbone leads to efficient, but not complete, energy transfer to the porphyrin sites, where sensitization of molecular oxygen to produce $^1O_2$ takes place. These materials do not cause toxicity toward cells in the dark as a result of the low pendant porphyrin content. Because of the light harvesting properties of the polymer backbone it is possible to attain higher levels of $^1O_2$ generation than when using similar concentrations of the porphyrin unit. These data demonstrate that the optical coupling in the polythiophene/porphyrin dyad translates into light dosages that are competitive with those of approved photosensitizers. Also noteworthy is that the residual polymer emission can be used to determine whether cancer cells are living or not, depending on the regions of highest intensities. By eliminating

non-specific electrostatic interactions and introducing folic acid to the backbone one finds that it is possible to retain all the useful optical properties of PTP and to achieve specific action toward folate receptor-overexpressed cancer cells. This collected set of observations and structure/function relationships indicate that conjugated polymer materials have the potential to act as multifunctional photosensitive agents for treating cancer infections and highlight the enormous potential offered by understanding the interactions of optically active conjugated polyelectrolytes with living cells.

4. Experimental Section

Materials: All chemicals were purchased from Acros, Aldrich Chemical Company or Alfa-Aesar and used as received. All organic solvent was purchased from Beijing Chemical Works and used as received. The disodium salt of 9,10-anthracenedipropionic acid (ADPA) was prepared according to the procedure in literature.[23] Ethidium bromide (EB) was purchased from Sigma. Pulmonary adenocarcinoma cell (A549) and renal cell carcinoma (A498), KB cancer cells and normal NIH 3T3 fibroblasts cells were purchased from cell culture center of Institute of Basic Medical Sciences, Chinese Academy of Medical Sciences (Beijing, China) and cultured in Dulbecco's Modified Eagle's Medium (DMEM) supplemented with 10% neonatal bovine serum (NBS), 4.0 mM glutamine and 4500 mg L^{-1} glucose. NBS was purchased from Sijiqing Biological Engineering Materials (Hangzhou, China). DMEM was purchased from HyClone/Thermofisher (Beijing, China). (3-(4,5-Dimethylthiazol-2-yl)-2,5-diphenyl-2H-tetrazolium hydrobromide) (MTT) was obtained from Xinjingke Biotech. (Beijing, China) and dissolved in 1×PBS before use. The water was purified using a Millipore filtration system.

Measurements: The absorbance for MTT analysis was recorded on a microplate reader (BIO-TEK Synergy HT) at a wavelength of 520 nm. The ^{1}H NMR and ^{13}C NMR spectra were recorded on a Bruker Avance 400 MHz spectrometer. Elemental analyses were carried out with a Flash EA1112 instrument. The fluorescence spectra were measured on a Hitachi F-4500 fluorometer with a Xenon lamp as excitation source. UV–vis absorption spectra were taken on a Jasco V-550 spectrometer. Phase contrast bright-field and fluorescence images were taken on a fluorescence microscope (Olympus 1 × 71) with a mercury lamp (100 W) as light source. The excitation wavelength was 540/40 nm for EB. Experiments for light-induced anticancer acitivty of cancer cells were performed with a metal halogen lamp (Mejiro Genossen MVL-210) that simulated a white light source. The wavelength was between 400 and 800 nm. The intensities of incident beams were checked by a power and energy meter and the 470nm light obtained by the type of 470/10 nm filter was used for PDT against cells.

*Synthesis of 5-[4-(6-Bromohexyloxy)phenyl]-10,15,20-tri-p-tolylporphyrin (**3**)*: The mixture of pyrrole (11.3 mmol), 4-(6-bromohexyloxy) benzaldehyde (**1**) (805 mg, 2.83 mmol) and *p*-tolualdehyde (**2**) (1.02 g, 8.49 mmol) in $CHCl_3$ (154 mL) was stirred for 15 min under nitrogen at room temperature, and then BF_3-diethyl ether (389 mg, 2.74 mmol) was added to this solution. After stirring for 1 h, DDQ (1.91 g, 8.42 mmol) was added and the reaction mixture was stirred for further 2 h at room temperature. Triethylamine (382 µL) was added and the crude mixture was passed through a silica column with petroleum ether/CH_2Cl_2 (1:1) as eluent. The residue was purified by a second silica column using petroleum ether/CH_2Cl_2 (2.3: 1) as the eluent to afford a purple powder (256 mg, 11%). ^{1}H NMR (400 MHz, $CDCl_3$, δ): 8.85 (s, 8H), 8.10–8.08 (d, 8H), 7.56–7.54 (d, 6H), 7.27–7.25 (d, 2H), 4.26–4.23 (t, 2H), 3.52–3.48 (t, 2H), 2.67 (s, 9H), 2.01–1.98 (m, 4H), 1.66–1.65 (m, 4H), –2.77(s, 2H); ^{13}C NMR (100 MHz, $CDCl_3$, δ): 158.9, 139.4, 137.4, 135.7, 134.6, 131.0, 127.5, 125.5, 120.2, 119.9, 112.7, 68.1, 34.0, 32.8, 29.4, 28.1, 25.6, 21.6. MS (MALDI-TOF) *m/z*: 837 $[M + H]^+$. Anal. calcd for $C_{53}H_{47}BrN_4O$: C 76.16, H 5.67, N 6.70; found: C 76.21, H 5.82, N 6.61.

*Synthesis of 4-(2-(Thiophen-3-yl)ethoxy)phenol (**5**)*: The mixture of hydroquinone (4.4 g, 40 mmol), K_2CO_3 (1.38 g, 10 mmol) and catalytic quantity of 18-crown-6 in air-free acetone (150 mL) was refluxed under nitrogen for 30 min and then 2-(3-thienyl)-ethanol tosylate (**4**) (564 mg, 2.0 mmol) was added. After refluxing under nitrogen for 24 h, the solvent was removed under reduced pressure and the residue was taken up in a mixture of CH_2Cl_2 and water. The organic layer was separated, washed with saturated aqueous $NaHCO_3$ and brine, and dried over anhydrous $MgSO_4$. After removal of the solvent, the residue was purified by silica gel chromatography using petroleum ether/EtOAC (80:1) as eluent to afford a clear light yellow oil (240 mg, 59%). ^{1}H NMR (400 MHz, $CDCl_3$, δ): 7.26 (m, 1H), 7.07 (s, 1H), 7.02–7.01 (d 1H), 6.79–6.73 (dd, 4H), 4.75 (s, 1H), 4.13–4.10 (t, 2H), 3.10-3.07 (t, 2H); ^{13}C NMR (100 MHz, $CDCl_3$, δ): 152.9, 149.9, 138.9, 128.8, 125.8, 121.8, 116.5, 116.3, 69.2, 30.5. EIMS *m/z*: 220 $[M^+]$. Anal. calcd for $C_{12}H_{12}O_2S$: C 65.43, H 5.49; found: C 64.88, H 5.59.

*Synthesis of Monomer **6***: A mixture of compound **5** (240 mg, 1.09 mmol), compound **3** (912 mg, 1.09 mmol), K_2CO_3 (300 mg, 2.18 mmol) and a catalytic amount of 18-crown-6 in DMF (50 mL) was stirred at 70 °C under nitrogen for 24 h. After cooling down to temperature, the solvent was removed under reduced pressure and the residue was washed with distilled water and extracted with dichloromethane. The organic layer was separated, washed with brine, and dried over anhydrous $MgSO_4$. After removal of the solvent, the residue was purified by silica gel chromatography using petroleum ether/EtOAC (40:1) as eluent to afford a purple powder (457 mg, 43%). ^{1}H NMR (400 MHz, $CDCl_3$, δ): 8.85 (s, 8H), 8.10–8.08 (d, 8H), 7.56–7.54(d, 6H), 7.26–7.22 (m, 2H), 7.07–7.02 (m, 2H), 6.86–6.82 (m, 3H), 6.58–6.54 (m, 2H), 4.25–3.99 (t, 6H), 3.10–3.08 (m, 2H), 2.70 (s, 9H), 2.01–1.89 (m, 4H), 1.68 (m, 4H), –2.76 (s, 2H); ^{13}C NMR (100 MHz, $CDCl_3$, δ): 158.9, 153.5, 152.9, 139.4, 138.7, 137.4, 135.7, 134.6, 131.4, 128.6, 127.5, 125.5, 121.5, 120.2, 119.9, 115.7, 115.5, 112.8, 68.8, 68.6, 68.2, 30.4, 29.5, 26.1, 21.6. MS (MALDI-TOF) *m/z*: 975 $[M^+]$. Anal. calcd for $C_{65}H_{58}N_4O_3S$: C 80.05, H 5.99, N 5.74; found: C 79.97, H 6.15, N 5.85.

*Synthesis of 3-(2-(6-Bromohexyloxy)ethyl)thiophene (**8**)*: 2-(Thiophen-3-yl)ethanol (663 µL, 6 mmol) was added to a suspension of sodium hydride (206 mg, 6 mmol) in dry DMF under N_2. After stirring for 30 min, 1,6-dibromohexane (4.6 mL, 10 mmol) was added to the solution by syringe at room temperature. After stirring overnight, the reaction was quenched by adding water. The mixture was extracted with CH_2Cl_2 three times. The combined organic layer was washed with brine and dried over $MgSO_4$, After removal of the solvent, the residue was purified by silica gel chromatography using petroleum ether/ethyl acetate (40:1) as eluent to afford compound 8 (0.54 g, 31%). ^{1}H NMR (400MHz, $CDCl_3$, δ) 7.37(m, 1H), 7.15–7.10 (m, 2H), 3.76 (t, 2H), 3.57 (t, 2H), 3.53 (t, 2H), 3.04 (t, 2H), 1.99 (m, 2H), 1.72(m, 2H), 1.61–1.45 (m, 4H); ^{13}C NMR (75MHz, $CDCl_3$, δ) 139.46; 128.53, 125.14, 121.04, 71.03, 70.77, 33.82, 32.79, 30.83, 29.57, 28.01, 25.43. HRMS (EI) *m/z*: $[M^+]$ calcd for $C_{12}H_{19}BrOS$, 290.0340; found, 290.0342.

*Synthesis of the Monomer 6-(2-(Thiophen-3-yl)ethoxy)hexyl trimethylammonium bromide (**9**)*: To a solution of compound **8** (291 mg, 1 mmol) in THF (0.5 mL) was added trimethylamine (3 mL). The mixture was allowed to stirrer at 40 °C overnight. Excessive trimethylamine and the solvent were removed under reduced pressure. The residue was dissolved in 1.0 mL of CH_3OH, and 10 mL of hexane was added to precipitate the product as a white solid (310 mg, 89%). ^{1}H NMR (400MHz, $CDCl_3$, δ) 7.27(m, 1H); 7.02-6.98(m, 2H), 3.65-3.56(m, 4H), 3.47(m, 11H), 2.91(t, 2H, 6.78), 1.75(br, 2H), 1.58(br, 2H), 1.42(br, 4H); ^{13}C NMR (75MHz, $CDCl_3$, δ) 139.34; 128.48, 125.10, 120.96, 70.79, 70.37, 66.64, 53.27, 30.61, 29.25, 25.81, 25.76, 23.02. ESIMS *m/z*: 270 $[M\text{-}Br]^+$. Anal. calcd for $C_{15}H_{28}BrNOS$: C 51.42, H 8.06, N 4.00; found C 51.11, H 7.95, N 4.12.

Synthesis of 5-[4-(6-n,n,n-Trimethylammoniumhexyloxy)phenyl]-10,15,20-tri-p-tolylporphyrin bromide (TPN): To a solution of compound **3** (60 mg, 0.072 mmol) in THF/$CHCl_3$ was added dropwise trimethylamine-methanol solution (3 mL), and the solution was stirred at 40 °C for 24 h. Excessive trimethylamine and the solvent were removed under reduced pressure. The residue was dissolved in CH_3OH (1 mL), and hexane (10 mL) was added to precipitate the product as a purple solid (51 mg, 79%). ^{1}H NMR (400 MHz, CD_3OD, δ): 8.84 (s, 8H), 8.09–8.07 (d, 8H), 7.54–

7.53(d, 6H), 7.24–7.22 (d, 2H), 4.21–4.19 (t, 2H), 3.69–3.64 (t, 2H), 3.44 (s, 9H), 2.69 (s, 9H) 1.96–1.93 (m, 2H), 1.85–1.81 (m, 2H),1.68–1.66 (m, 2H), 1.55–1.53 (m, 2H), –2.78(s, 2H). ESIMS *m/z*: 815 $[M\text{-}Br]^+$.

Synthesis of PT: A suspension of anhydrous $FeCl_3$ (65 mg, 0.4 mmol) in $CHCl_3$ (8 mL) was stirred for 30 min at room temperature under N_2. To this suspension was added a solution of monomer **9** (35 mg, 0.1 mmol) in $CHCl_3$ (10 mL), and the resulting solution was stirred for 2 days at room temperature. After the reaction was quenched by the addition of methanol, the precipitate was filtered off and the pellet was washed by CH_3OH. The precipitate was dissolved in DMSO/H_2O (1:10) and then dialyzed through a membrane with a molecular weight cutoff of 3500 for 2 days to yield a yellow solid (16 mg). ^{1}H NMR (400 MHz, DMSO-d_6, δ): 7.75-7.31(br), 3.32 (br), 3.08-2.51 (br), 1.52-1.25 (br).

Synthesis of PTP: A suspension of anhydrous $FeCl_3$ (130 mg, 0.8 mmol) in $CHCl_3$ (15 mL) was stirred for 30 min at room temperature under N_2. To this suspension was added a solution of monomer **6** (33 mg, 0.033 mmol) and monomer **9** (135 mg, 0.386 mmol) in $CHCl_3$ (10 mL), and the resulting solution was stirred for 2 days at room temperature. After the reaction was quenched by the addition of methanol, the precipitate was filtered off and the pellet was washed repeatedly by CH_3OH. The precipitate was dissolved in DMSO/H_2O (1:10) and then dialyzed through a membrane with a molecular weight cutoff of 3500 for 3 days to yield a yellow solid (11 mg). ^{1}H NMR (400 MHz, DMSO-d_6, δ): 7.31(br), 3.70 (br), 3.44-3.31 (br), 3.08–2.67 (br), 1.65-1.54(br), 1.34-1.24 (br).

*Synthesis of 5-[4-(6-(4-Hydroxyphenoxy)hexyloxy)phenyl]-10,15,20-tri-p-tolyl porphyrin (**10**)*: A mixture of hydroquinone (329 mg, 2.99 mmol), K_2CO_3 (166 mg, 1.2 mmol) and catalytic quantity of 18-crown-6 in air-free DMF (10 mL) was heated at 70 °C for 30 min and then compound **3** (100 mg, 0.12 mmol) was added. After further reaction for 20 h, the solvent was removed under reduced pressure and the residue was taken up in a mixture of CH_2Cl_2 and water. The organic layer was separated, washed with brine, and dried over anhydrous $MgSO_4$. After removal of the solvent, the residue was purified by silica gel chromatography using petroleum ether/EtOAc (6:1) as eluent to afford a purple powder (55 mg, 53.4%). ^{1}H NMR (400 MHz, $CDCl_3$, δ): 8.95 (s, 8H), 8.20–8.18 (d, 8H), 7.65–7.63(d, 6H), 7.35 (m, 2H), 6.92–6.90(d, 2H), 6.84–6.82(d, 2H), 4.56(s, 1H) 4.33 (t, 2H), 4.08–4.05 (t, 2H), 2.79 (s, 9H), 2.09–1.96 (m, 4H), 1.76 (m, 4H), –2.67(s, 2H); ^{13}C NMR (100 MHz, $CDCl_3$, δ): 158.9, 153.4, 149.5, 139.4, 137.4, 135.7, 134.6, 131.0, 127.5, 120.1, 119.9, 116.1, 115.7, 112.8, 68.7, 68.2, 29.8, 29.5, 26.1, 21.6. MS (MALDI-TOF) *m/z*: 865 $[M]^+$. Anal. calcd for $C_{59}H_{52}N_4O_3$: C 81.92, H 6.06, N 6.48; found C 81.06, H 6.04, N 6.71.

*Synthesis of Compound **12***: A mixture of compound **10** (30 mg, 0.035 mmol), compound **11** (71 mg, 0.104 mmol), K_2CO_3 (48 mg, 0.35 mmol) and a catalytic amount of 18-crown-6 in air-free DMF (10 mL) was heated at 70 °C under nitrogen for 20 h. After cooling down to room temperature, the solvent was removed under reduced pressure and the residue was washed with distilled water and extracted with dichloromethane. The organic layer was separated, washed with brine, and dried over anhydrous $MgSO_4$. After removal of the solvent, the residue was purified by silica gel chromatography using petroleum ether/EtOAc (6:1) as eluent to afford a purple powder (21 mg, 43.8%). ^{1}H NMR (400 MHz, $CDCl_3$, δ): 8.85 (s, 8H), 8.10–8.09 (d, 8H), 7.56-7.54(d, 6H), 7.26–7.22 (m, 2H), 6.86–6.83 (m, 5H), 4.32–4.24 (m, 4H), 3.81–3.67 (m, 16H), 2.70 (s, 9H), 2.02–1.89 (m, 4H), 1.72–1.68 (m, 4H), –2.77(s, 2H). MS (MALDI-TOF) *m/z*: 1375 $[M]^+$, 1249 $[M\text{-}I]^+$.

*Synthesis of Polymer **15***: A mixture of monomer **12** (28 mg, 0.0206 mmol), *tert*-butyl 6-(2-(2,5-dibromothiophen-3-yl)ethoxy)hexylcarbamate **13** (100 mg, 0.2062 mmol) and 5,5-dimethyl-2-(5-(5,5-dimethyl-1,3,2-dioxaborinan-2-yl)thiophen-2-yl)-1,3,2-dioxaborinane **14** (70 mg, 0.227 mmol) in toluene (4 mL) and 2.0 M potassium carbonate (2 mL) was degassed and then a catalytic amount of Pd(dppf)Cl_2 was added. The resulting mixture was stirred at 85 °C for 2 days under nitrogen. After cooling down to room temperature, water (20 mL) was added and the mixture was extracted with $CHCl_3$. The organic layer was dried over anhydrous MgSO4 and the solvent was removed. The crude product was redissolved in $CHCl_3$ (0.5 mL) and then precipitated in CH_3OH. The precipitate was collected by centrifugation. The precipitate was dissolved in DMSO/H_2O (1:10) and then dialyzed through a membrane with a molecular weight cutoff of 3500 for 3 days to yield of polymer 15 (12 mg). ^{1}H NMR (400 MHz, $CDCl_3$, δ): δ (ppm) 8.85 (br), 8.09 (br), 7.54 (br), 7.00 (br), 6.84(br,), 4.26 (br), 3.97 (br), 3.43 (br), 3.06 (br), 2.70 (br), 2.14 (br),1.87 (br), 1.56 (br), 1.43 (br),1.32 (br), 1.25 (br), 0.83 (br).

Synthesis of Polymer PTPF: To a solution of polymer **15** (7 mg) in $CHCl_3$ (2.0 mL) was added trifluoroacetic acid (1 mL) and then stirred at room temperature overnight. The solvent was removed under reduced pressure. The residue was redissolved in methanol/$CHCl_3$ (5 mL, v/v 1:3) and triethylamine (1 mL) was added. After stirring overnight, the solvents were removed at reduced pressure. The residue was dissolved in DMSO (1 mL), then a solution of folic acid **16** (0.66 mg, 0.0015 mmol), *N*-hydroxysuccinimide (0.35 mg, 0.003 mmol) and EDCI (0.56 mg, 0.003 mmol) in DMSO (2.0 mL) was dropwise added. The resulting solution was stirred at room temperature for 2 days in dark. A brown solid (4.0 mg) was obtained after dialysis through a membrane with a molecular weight cutoff of 3500 for 2 days in water under nitrogen. ^{1}H NMR (400 MHz, DMSO-d_6, δ): 8.83 (br), 8.09 (br), 7.64 (br), 7.50 (br), 7.35 (br), 7.19(br), 6.88–6.80(br), 6.65(br), 5.32(br), 4.25 (br), 3.97 (br), 3.90 (br), 3.70 (br), 3.49 (br), 2.94(br), 2.64 (br), 2.13 (br), 2.30 (br), 1.99 (br), 1.62 (br), 1.38 (br), 1.23 (br), 0.88 (br).

Singlet Oxygen Measurement: To 300 μL of the aqueous solutions of PTP, PT or TPN were added 6 μL of ADPA solution in water (6 mM). D_2O was used to replace H_2O in these experiments. The UV–vis absorption spectra were measured at 1.0 min intervals after the samples were irradiated with white light and the reduction in absorption of ADPA at 378 nm was plotted as a function of the irradiation time.

Cell Viability Assay by MTT: A498 cells and A549 cells were routinely grown in DMEM (high glucose) medium containing 10% NBS. All cell lines were harvested for subculture using trypsin (0.05%, Gibco/Invitrogen) and grown in a humidified atmosphere containing 5% CO_2 and 95% air at 37 °C. Cells were subcultured in 96-well plates the day before the experiment at a density of $4 - 7 \times 10^4$ cells per well, and then cultured for 24 h. PTP, PT, TPN with varying concentrations were respectively added into the cells followed by further culture for 24 h. The culture media were discarded and fresh cell growth medium (100 μL) was added. PDT treatment was performed by using he 470 nm light obtained by the type of 470/10 nm filter with a dose of 2.5 J ·cm^{-2} at a fluence rate of 1.4 mW·cm^{-2} for 30 min of irradiation. The cells were allowed to continue growth for 24h, at which time the the culture media were discarded and MTT (1 mg mL^{-1}, 100 μL per well) was added to the wells followed by incubation at 37 °C for 4 h. The supernatant was abandoned, and DMSO (150 μL) per well was added to dissolve the produced formazan and the plates were shaken for an additional 10 min The absorbance values of the wells were then read with microplate reader at a wavelength of 520 nm. The cell viability rate (VR) was calculated according to the following equation where the control group was carried out in the absence of photosensitizers.[26] The MTT assays of KB cancer cells which were cultured in folate-free RPMI 1640 medium containing 10% NBS and normal NIH 3T3 fibroblasts cells which were cultured in DMEM (high glucose) medium containing 10% NBS in the presence of PTPF were performed using the procedures described above.

$$VR(\%) = \frac{A_{\text{experimental group}}}{A_{\text{control group}}} \times 100\%$$

In Vitro Imaging of Photoinduced Death of A498 Cells by PTP: The A498 cells were seeded in 35 mm culture plates (Nunc) at a density of approximately 8×10^4 cells per plate for 24 h, and then the cells were washed once with 1 × PBS and then grown in DMEM medium (1 mL) with 10 μM PTP. After the cells were further cultured for 12 h, then the culture media were discarded and fresh DMEM medium was added. The plates were irradiated under 470 nm light for 0, 10 and 30 min respectively, then ethidium bromide (EB) was added to the samples that had been illuminated by light, and they were then observed by fluorescence microscopy. Upon addition of EB to the samples, the phase contrast images were taken at 100 ms and the fluorescence images were taken at 300 ms under PTP and under EB filters. The false color of PTP is yellow

and the type of light filter is D455/70 nm exciter, 500 nm beamsplitter, and D525/30 nm emitter. The false color of EB is red and the type of light filter is D540/40 nm exciter, 570 nm beamsplitter, and D600/50 nm emitter.

Acknowledgements

The authors are grateful for the National Natural Science Foundation of China (No. 20725308, 21033010, 21021091, 90913014), the Major Research Plan of China (No. 2011CB932302, 2011CB935800), the National Science Foundation (DMR 1005546), the ITC-PAC (Contract No. FA5209-08-P-0365) and the Institute for Collaborative Biotechnologies at the University of California, Santa Barbara.

Received: April 16, 2011
Revised: July 20, 2011
Published online: September 15, 2011

[1] T. M. Swager, *Acc. Chem. Res.* **1998**, *31*, 201–207.
[2] B. Liu, G. C. Bazan, *Chem. Mater.* **2004**, *16*, 4467–4476.
[3] J. R. Lakowicz, *Principles of Fluorescence Spectroscopy*, Kluwer Academic/Plenum, New York **1999**.
[4] B. Liu, G. C. Bazan, *J. Am. Chem. Soc.* **2006**, *128*, 1188–1196.
[5] S.W. Thomas III, G. D. Joly, T. M. Swager, *Chem. Rev.* **2007**, *107*, 1339–1386.
[6] H. A. Ho, A. Najari, M. Leclerc, *Acc. Chem. Res.* **2008**, *41*, 168–178.
[7] X. Duan, L. Liu, F. Feng, S. Wang, *Acc. Chem. Res.* **2010**, *43*, 260–270.
[8] U. H. F. Bunz, V. M. Rotello, *Angew. Chem. Int. Ed.* **2010**, *49*, 3268–3279.
[9] K. E. Achyuthan, T. S. Bergstedt, L. Chen, R. M. Jones, S. Kumaraswamy, S. A. Kushon, K. D. Ley, L. Lu, D. McBranch, H. Mukundan, F. Rininsland, X. Shi, W. Xia, D. G. Whitten, *J. Mater. Chem.* **2005**, *15*, 2648–2656.
[10] H. Jiang, P. Taranekar, J. R. Reynolds, K. S. Schanze, *Angew. Chem. Int. Ed.* **2009**, *48*, 4300–4316.
[11] C. Wu, B. Bull, K. Christensen, J. McNeill, *Angew. Chem. Int. Ed.* **2009**, *48*, 2741–2745.
[12] C. L. Wu, Q. H. Xu, *Macromol. Rapid Commun.* **2009**, *30*, 504–508.
[13] M. A. Oar, W. R. Dichtel, J. M. Serin, J. M. J. Fréchet, J. E. Rogers, J. E. Slagle, P. A. Fleitz, L.-S. Tan, T. Y. Ohulchanskyy, P. N. Prasad, *Chem. Mater.* **2006**, *18*, 3682–3692.
[14] C.-Y. Chen, Y. Tian, Y.-J. Cheng, A. C. Young, J.-W. Ka, A. K.-Y. Jen, *J. Am. Chem. Soc.* **2007**, *129*, 7220–7221.
[15] C. Xing, Q. Xu, H. Tang, L. Liu, S. Wang, *J. Am. Chem. Soc.* **2009**, *131*, 13117–13124.
[16] J. P. Celli, B. Q. Spring, I. Rizvi, C. L. Evans, K. S. Samkoe, S. Verma, B. W. Pogue, T. Hasan, *Chem. Rev.* **2010**, *110*, 2795–2838.
[17] D. E. Dolmans, D. Fukumura, R. K. Jain, *Nat. Rev. Cancer* **2003**, *3*, 380–387.
[18] L. Lu, F. H. Rininsland, S. K. Wittenburg, K. E. Achyuthan, D. W. McBranch, D. G. Whitten, *Langmuir* **2005**, *21*, 10154–10159.
[19] T. S. Corbitt, J. R. Sommer, S. Chemburu, K. Ogawa, L. K. Ista, G. P. Lopez, D. G. Whitten, K. S. Schanze, *Appl. Mater. Interfaces* **2009**, *1*, 48–52.
[20] O.-K. Kim, J. Je, J. S. Melinger, *J. Am. Chem. Soc.* **2006**, *128*, 4532–4533.
[21] C. Wu, B. Bull, C. Szymanski, K. Christensen, J. McNeill, *ACS Nano.* **2008**, *2*, 2415–2423.
[22] X. Feng, Y. Tang, X. Duan, L. Liu, S. Wang, *J. Mater. Chem.* **2010**, *20*, 1312–1316.
[23] B. A. Lindig, M. A. J. Rodgers, A. P. Schaap, *J. Am. Chem. Soc.* **1980**, *102*, 5590–5593.
[24] E. Buytaert, M. Dewaele, P. Agostinis, *Biochim. Biophys. Acta.* **2007**, *1776*, 86–107.
[25] D. W. Nicholson, *Nature* **2000**, *407*, 810–816.
[26] Z. Darzynkiewicz, *Cytometry* **1997**, *27*, 1–20.
[27] F. Denizot, R. Lang, *J. Immunol. Methods* **1986**, *89*, 271–277.
[28] R. Jendželovský, J. Mikeš, Ján Koval', K. Souček, J. Procházková, M. Kello, V. Sačková, J. Hofmanová, A. Kozubík, P. Fedoročko, *Photochem. Photobiol. Sci.* **2009**, *8*, 1716–1723.
[29] H. B. Ris, H. J. Altermatt, R. Inderbitzi, *Br. J. Cancer* **1991**, *64*, 1116–1120.
[30] M. McHugh, Y. C. Cheng, *J. Biol. Chem.* **1979**, *254*, 11312–11318.